Experimental Brain Research (2024) 242:477–490
https://doi.org/10.1007/s00221-023-06764-w

RESEARCH ARTICLE

Desflurane improves electrical activity of neurons and alleviates oxygen–glucose deprivation-induced neuronal injury by activating the Kcna1-dependent Kv1.1 channel

Xiaolei Ni[1] · Xiaoyan Yu[1] · Qingqing Ye[1] · Xiaohu Su[1] · Shuai Shen[1]

Received: 12 September 2023 / Accepted: 11 December 2023 / Published online: 7 January 2024

Abstract

Several volatile anesthetics have presented neuroprotective functions in ischemic injury. This study investigates the effect of desflurane (Des) on neurons following oxygen–glucose deprivation (OGD) challenge and explores the underpinning mechanism. Mouse neurons HT22 were subjected to OGD, which significantly reduced cell viability, increased lactate dehydrogenase release, and promoted cell apoptosis. In addition, the OGD condition increased oxidative stress in HT22 cells, as manifested by increased ROS and MDA contents, decreased SOD activity and GSH/GSSG ratio, and reduced nuclear protein level of Nrf2. Notably, the oxidative stress and neuronal apoptosis were substantially blocked by Des treatment. Bioinformatics suggested potassium voltage-gated channel subfamily A member 1 (Kcna1) as a target of Des. Indeed, the Kcna1 expression in HT22 cells was decreased by OGD but restored by Des treatment. Artificial knockdown of Kcna1 negated the neuroprotective effects of Des. By upregulating Kcna1, Des activated the Kv1.1 channel, therefore enhancing K^+ currents and inducing neuronal repolarization. Pharmacological inhibition of the Kv1.1 channel reversed the protective effects of Des against OGD-induced injury. Collectively, this study demonstrates that Des improves electrical activity of neurons and alleviates OGD-induced neuronal injury by activating the Kcna1-dependent Kv1.1 channel.

Keywords Oxygen–glucose deprivation · Desflurane · Kcna1 · Neuronal firing · Kv1.1 channel

Introduction

Ischemic stroke stands as the second leading cause of mortality and a significant contributor to global disability, and its incidence is increasing with an aging population (Katan and Luft 2018). This condition refers to a clinical syndrome where blood circulation in the brain is disrupted due to vessel occlusion, leading to varying degrees of oxygen–glucose deprivation (OGD) and immediate neurological impairment (Miller et al. 2016; Morone and Pichiorri 2023). While recombinant tissue plasminogen activator remains the most effective treatment for inducing thrombolysis in ischemic stroke, its use is restricted by a narrow time window (within 3–4.5 h after onset) and potential complications (Robinson et al. 2011; Zhong et al. 2019). The considerable mortality and disability caused by stroke have garnered substantial interest from researchers and clinicians in seeking more efficient and safer treatments, especially for patients ineligible for thrombolytic therapy.

Neuronal death, predominantly occurring in the ischemic penumbra surrounding the infarct area, represents a primary pathological occurrence consequent to ischemic stroke, significantly influencing mortality and disability rates (Li et al. 2014; Mao et al. 2022). Initially, neuronal apoptosis is instigated by calcium influx, impairment of mitochondria, depletion of energy, and glutamate excitotoxicity resulting from OGD (Hao et al. 2014). Due to the brain tissue's limited antioxidant defenses, the subsequent production of oxygen free radicals, nitric oxide, and reactive oxygen species (ROS) leads to secondary harm to the neurons (Hao et al. 2014; Lakhan et al. 2009). A promising approach to enhance the prognosis of ischemic stroke involves the prevention of neuronal injury or uncontrolled neuronal death.

Communicated by Sreedharan Sajikumar.

✉ Shuai Shen
Shenshuai271@163.com

[1] Department of Anesthesiology and Perioperative Medicine, The Affiliated Suqian First People's Hospital of Nanjing Medical University, No. 120, Suzhi Road, Sucheng District, Suqian 223800, Jiangsu, People's Republic of China

Several volatile anesthetics, such as isoflurane (Khatibi et al. 2011) and sevoflurane (Cheng et al. 2019), have shown neuro-protective properties in ischemic stroke and OGD models. Desflurane (Des) is among the common volatile anesthetics, exhibiting the potential to shield cerebral tissue against detrimental occurrences such as apoptosis, inflammation, degeneration, energy failure, and inflammation (Schifilliti et al. 2010). While safety concerns have been raised regarding volatile anesthetics, including Des, and their potential impact on cardiovascular, central nervous system, and respiratory functions (Brioni et al. 2017), existing evidence also suggests that Des is not significantly associated with cardiac side effects (Malhotra et al. 2013; Vizuete et al. 2012). Additionally, Des offers other advantages such as rapid induction, a pleasant smell, and rapid postoperative recovery (Kumar et al. 2023). Nonetheless, the precise functions of Des in neurons following ischemic stroke or OGD remain an enigma. By performing comprehensive bioinformatics analyses in this study, we identified potassium voltage-gated channel subfamily A member 1 (Kcna1) as an auspicious promising target of Des, presenting dysregulation within neurons after OGD. Voltage-gated potassium (Kv) channels boast widespread distribution across the central and peripheral nervous systems, orchestrating potassium ion (K^+) currents pivotal for membrane repolarization and hyperpolarization, thereby generally imposing constraints upon neuronal excitability (Shah and Aizenman 2014). The Kcna1 gene encodes α subunits of the Kv1.1 channel, playing a critical role in sustaining appropriate neuronal firing patterns and forestalling hyperexcitability (Paulhus and Glasscock 2023). Under circumstances of pathophysiology, an excessively heightened state of excitation might potentially culminate in excitotoxic death. (Bhat et al. 2022). This study aims to determine the neuroprotective effect of Des after OGD and investigate the involvement of the Kcna1/Kv1.1 channel and neuronal electrophysiology.

Materials and methods

Cell model of OGD and Des treatment

The immortalized mouse hippocampal neuron cell line HT22 (CL-0697, Procell Life Science & Technology Co., Ltd., Wuhan, Hubei, China) was incubated in DMEM (12100046, Thermo Fisher Scientific, Rockford, IL, USA) containing 10% fetal bovine serum and 1% antibiotic–antimycotic at 37 °C with 5% CO_2. When cells reached 70–80% confluence, they were washed with phosphate-buffered saline (PBS), transferred into serum-free medium, and cultured in an incubator enriched with 94% N_2, 5% CO_2, and 1% O_2 at 37 °C for 8 h to generate OGD-induced injury. For cells that were assigned for Des treatment, Des was pumped into the incubator at a rate of 0.5 L/min during the last 2 h of the OGD process. In addition, another group of Des pretreatment was set (pre-Des), where cells were pre-treated with Des for 2 h before OGD challenge.

Pre-transfection and pre-treatment of cells before OGD

Three short hairpin (sh) RNA plasmids of Kcna1 (sh-RNA 1#, sh-RNA 2#, and sh-RNA 3#) were procured from VectorBuilder Inc. (Guangzhou, Guangdong, China) and transfected into the HT22 cells using Lipofectamine 3000 (Thermo Fisher Scientific). After incubation at 37 °C with 5% CO_2 for 48 h, the cells were transferred into fresh culture medium, and the knockdown efficacy of shRNAs was analyzed using reverse transcription quantitative polymerase chain reaction (RT-qPCR). The one with the greatest knockdown efficacy was selected for subsequent use. For artificial inhibition of the Kv1.1 channel, the HT22 cells were treated with 100 nM of Dendrotoxin K (Dtx-K) (T76187, Topscience Co. Ltd., Shanghai, China) for 30 min.

Cell counting kit-8 (CCK-8) method

According to the instructions of a CCK-8 kit (HY-K0301, MedChemExpress, Monmouth Junction, NJ, USA), the HT22 cells were seeded in 96-well plates at 5000 cells per well. Then, each well was added with 10 µL CCK-8 reagent for 2 h of cell incubation at 37 ℃.

Terminal deoxynucleotidyl transferase (TdT)-mediated dUTP nick end labeling (TUNEL)

Apoptosis of the HT22 cells was analyzed using a TUNEL cell apoptosis detection kit (C1086, Beyotime Biotechnology Co., Ltd, Shanghai, China). In short, the cells were seeded in 96-well plates at 3000 cells per well. The cells were then washed wish PBS and labeled with 50 µL TUNEL reagent and 4′, 6-diamidino-2-phenylindole (DAPI) at 37 ℃ in the dark for 60 min. The labeling was then observed under a fluorescent microscope.

Lactate dehydrogenase (LDH) detection

The LDH content in cells was examined using an LDH detection kit (11644793001, Sigma-Aldrich, Merck KGaA, Darfmstadt, Germany). In brief, the HT22 cells were seeded in 96-well plates and added with 150 µL of diluted LDH release reagent until fully mixed. After 1 h of incubation, the cells were centrifuged, and 120 µL of supernatant was transferred into the wells of another 96-well plate, followed by the addition of 60 µL of LDH working solution for a dark incubation at room temperature for 30 min. The optical

density (OD) at 490 nm was measured. After the removal of culture solution, the remaining cells were lysed by 100% Triton X-100. The LDH releasing rate was calculated as follows: rate = secretory LDH × 100/secretory LDH + intracellular LDH in Triton X-100-treated cells.

Measurement of ROS

The ROS level in cells was determined using an ROS detection kit (S0033S, Beyotime). In short, the cells were seeded in 96-well plates and incubated with diluted dichlorofluorescein diacetate solution at 37 ℃ for 20 min. Then, the cells were washed with serum-free medium, and the fluorescence signal in cells was determined under a fluorescent microscope.

Measurement of malondialdehyde (MDA) content and superoxide dismutase (SOD) activity

MDA content in cells was measured using an MDA detection kit (BC0025, Solarbio Science & Technology Co., Ltd., Beijing, China). In short, the HT22 cells were lysed and centrifuged. Then, 0.1 mL of supernatant was collected and mixed with 0.3 mL of MDA detection solution in a 100 ℃-water bath for 60 min. Then, the sample was cooled down and centrifuged, and 200 μL of supernatant was added to 96-well plates. The MDA content was measured by detecting the OD values at 532 and 600 nm, respectively, using a microplate reader.

The SOD activity was analyzed using the SOD detection kit (S0101M, Beyotime). In brief, the HT22 cells were lysed and centrifuged, and the supernatant was collected and incubated with WST-8 working solution and initial reaction reagent at 37 ℃ for 30 min. The OD value at 450 nm was read to evaluate the SOD activity.

Measurement of the ratio of reduced glutathione (GSH) to oxidized glutathione (GSSG)

The GSH/GSSG ratio in cells was measured using a GSH and GSSG assay kit (MAK440, Sigma-Aldrich). In short, the cells were washed with PBS and centrifuged to collect the sediment. The protein removal reagent M solution in a volume three times that of the sediment was added. Then, the cells were seeded on 96-well plates and incubated with 150 μL of total GSH detection working solution at room temperature for 5 min, followed by the addition of 50 μL of nicotinamide adenine dinucleotide phosphate solution (0.5 mg/mL). After 25 min of reaction, the OD value at 412 nm was detected.

Isolation of nuclear protein

According to the instructions of the nuclear and cytoplasmic protein extraction kit (78833, Thermo Fisher Scientific), the HT22 cells were washed and centrifuged to discard the supernatant. The sediment was collected, to which 50 μL of PMSF-containing nuclear protein extraction reagent was added, followed by a high-speed vortex for 15–30 s. The vortex was performed at a 2-min interval within 30 min. Then, the sample was centrifuged at 12,000*g* at 4 ℃ for 10 min, and the supernatant was collected, which was the nuclear protein. The nuclear protein level of nuclear factor erythroid 2-related factor 2 (Nrf2) was examined using western blot (WB) analysis with Histone-3 used as the endogenous control.

WB analysis

The HT22 cells were lysed in RIPA lysis buffer to extract total protein, and the protein concentration was determined using a bicinchoninic acid kit. The total protein sample, or the nuclear protein sample mentioned above, was separated by 8–10% SDS-PAGE and loaded onto polyvinylidene fluoride membranes. The membranes were blocked by 1% nonfat milk and probed with the antibodies of Kcna1 (1:1000, A16906, ABclonal Biotech Co. Ltd., Hubei, China), B-cell lymphoma-2 (Bcl-2, 1:2000, ab182858, Abcam Inc., Cambridge, MA, USA), Bcl-2-associated X (Bax, 1:1000, ab32503, Abcam), β-actin (1:5000, ab8227, Abcam), Histone-3 (1:1000, ab1791, Abcam), and Nrf2 (1:1000, GTX103322, GeneTex Inc., San Antonio, TX, USA) at 4 ℃ overnight. After the removal of excess antibodies, the membranes were incubated with HRP-conjugated goat anti-rabbit IgG (1:2000, ab6721, Abcam) at room temperature for 1 h. The protein bands were developed using enhanced chemiluminescence, and relative level of target proteins was determined using Image J by analyzing the gray values.

RNA quantification

Total RNA from HT22 cells was extracted using the TRIzol reagent, which was used to synthesize cDNA using a HiScript reverse transcription kit (R302-01, Vazyme Biotech Co., Ltd, Nanjing, Jiangsu, China). The cDNA was then applied for real-time qPCR analysis using the SYBR Green qPCR Master Mix (MedChemExpress) on the ABI StepOne real-time qPCR system (4376357, Thermo Fisher Scientific). Expression of Kcna1 mRNA in cells relative to β-actin mRNA is examined by the $2^{-\Delta\Delta Ct}$ method. The primer sequences included: Kcna1 (F) 5′-GAGTCGCACTTCTCCAGTATCC-3′, Kcna1 (R) 5′-CCCACGATCTTGCCTCCAATTG-3′; and β-actin (F) 5′-CATTGCTGACAGGATGCAGAAGG-3′, β-actin (R) 5′-TGCTGGAAGGTGGACAGTGAGG-3′.

Electrophysiological analysis

The whole-cell patch-clamp technique was used to record the neuronal electrical activity at room temperature using AXON 700B and Digidata 1550. The bath solution consisted of 140 mM NaCl, 5 mM KCl, 2 mM $MgCl_2$, 2 mM $CaCl_2$, 10 mM HEPES, and 10 mM glucose (pH adjusted to 7.4 with NaOH). The pipette (4–6 MΩ) was filled with the intracellular solution containing 140 mM CsCl, 5 mM EGTA, and 10 mM HEPES (pH adjusted to 7.2 with CsOH). Throughout the experiment, the series resistance was monitored and typically kept below 20 MΩ. Electrophysiological data were filtered at 1.0 kHz and digitized at 50 kHz.

For the detection of K^+ currents, the pipette solution contained 120 mM L-aspartic acid, 20 mM KCl, 1 mM $MgCl_2$, 5 mM BAPTA, 5 mM HEPES, and 35 mM mannitol (pH adjusted to 7.2 with KOH). Data were only collected for analysis when the resting membrane potential (RMP) of the cell was more negative than −35 mV.

Assessment of intracellular Ca^{2+} levels

Intracellular Ca^{2+} levels in HT22 cells were examined using the Ca^{2+} binding dye Fluo-3 AM (F8840, Solarbio). Cells were incubated with 5 μM Fluo-3 AM (diluted in HBSS solution) at 37 °C for 30 min. Subsequently, the Fluo-3 AM working solution was removed, and cells were washed with HEPES buffer saline. Cells were then incubated at 37 °C for an additional 30 min in HBSS solution containing 1% fetal bovine serum. Images were obtained using fluorescence microscopy (Leica Biosystems, Shanghai, China), and Image J software was utilized to assess the relative fluorescence intensity of cells for the analysis of intracellular Ca^{2+} concentration.

Statistical analysis

All data were collected from no less than three independent experiments and analyzed using Prism 8.0.2 (GraphPad, La Jolla, CA, USA). Differences between groups were analyzed using the Student's *t* test or the one- or two-way analysis of variance (ANOVA), as appropriate. $p < 0.05$ was considered statistically significant.

Results

Des treatment alleviates OGD-induced injury in HT22 cells

A cell model of OGD-induced injury was generated. As expected, OGD significantly decreased the viability of HT22 cells (Fig. 1A) while increasing the LDH release (Fig. 1B), and it led to significant cell atrophy (Fig. 1C). This evidence suggests the successful modeling. Importantly, the Des treatment restored the cell viability (with no significant difference compared to the Control group), decreased LDH release (still showing a significant increase compared to the Control group), and improved the cell morphology (Fig. 1A–C). Furthermore, the TUNEL assay showed that the apoptosis of cells was increased following OGD but decreased by the Des treatment (still showing a significant increase compared to the Control group) (Fig. 1D). Concordantly, the OGD procedure increased the level of pro-apoptotic protein Bax while reducing the level of anti-apoptotic Bcl-2. These changes were largely reversed by the Des treatment as well (with the Bax level still showing a significant difference compared to the Control group, while the Bcl-2 level no longer showed a significant difference compared to the Control group) (Fig. 1E). Notably, when Des was administered prior to the OGD challenge, the pre-treatment regimen did not present a significant preventive effect of Des against OGD-induced neuronal death (Fig. 1F–G). This evidence demonstrates that Des is more likely to exert an alleviating effect rather than a preventive effect against OGD-induced neuronal damage.

Des alleviates OGD-induced oxidative stress in neurons

Oxidative stress plays a crucial role in neuronal damage and apoptosis in ischemic conditions. Indeed, we found that the OGD procedure led to significantly increased ROS and MDA contents in HT22 cells (Fig. 2A and B), reduced the GSH/GSSG ratio (Fig. 2C), and decreased the SOD activity (Fig. 2D). The Des treatment rescued the anti-oxidant defense in cells, as manifested by decreased ROS and MDA contents and restored GSH/GSSG ratio and SOD activity (with the ROS and MDA contents still showing a significant increase compared to the Control group, while the GSH/GSSG ratio and SOD activity no longer showed a significant difference). When measuring the expression of Nrf2, a key transcription factor involved in maintaining redox homeostasis, we found that the nuclear protein level of Nrf2 in of HT22 cells was slightly upregulated following OGD procedure and further substantially activated following Des treatment (Fig. 2E), indicating the activation of the anti-oxidant defense mechanism.

Des restores Kcna1 expression decreased by OGD

To unravel the molecular mechanism underpinning the neuron-protective roles of Des, we predicted the possible downstream proteins of Des based on its chemical structure

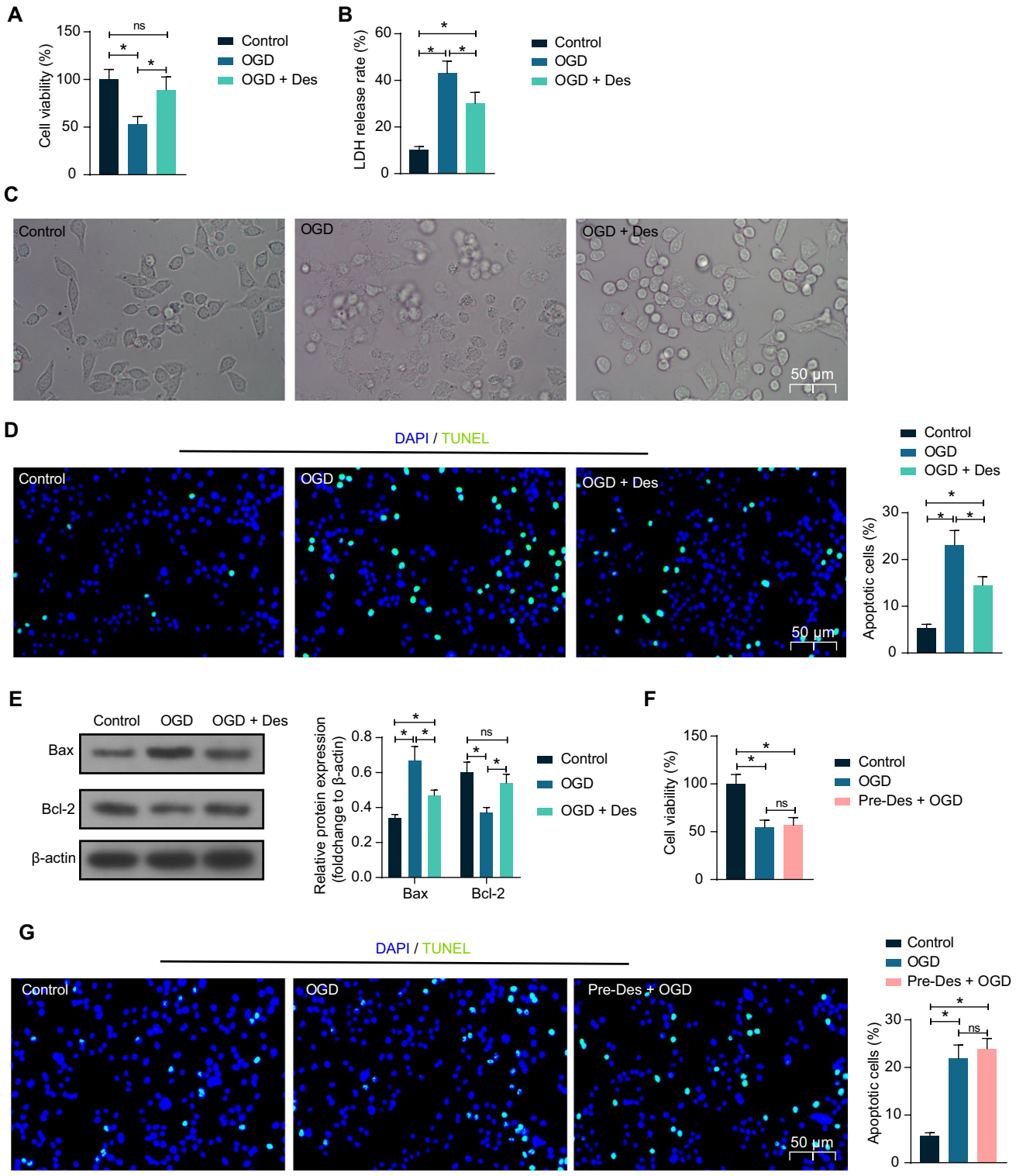

Fig. 1 Des treatment alleviates OGD-induced injury in HT22 cells. HT22 neuronal cells were subjected to OGD and then treated with Des. **A** viability of HT22 cells measured by CCK-8 assay; **B** LDH release in cells to analyze the cytotoxicity; **C** morphologic alterations in cells observed under microscopy; **D** apoptosis of cells analyzed using TUNEL assay; **E** protein levels of Bax and Bcl-2 in cells determined using WB analysis. Another pre-Des group was set where HT22 cells were pre-treated with Des for 2 h, followed by OGD challenge. **F** viability of HT22 cells measured by CCK-8 assay; **G** apoptosis of cells analyzed using TUNEL assay. Differences were analyzed using one-way (**A**, **B**, **D**, **F**, and **G**) or two-way ANOVA (**E**). *$p < 0.05$, ns denotes to no significance

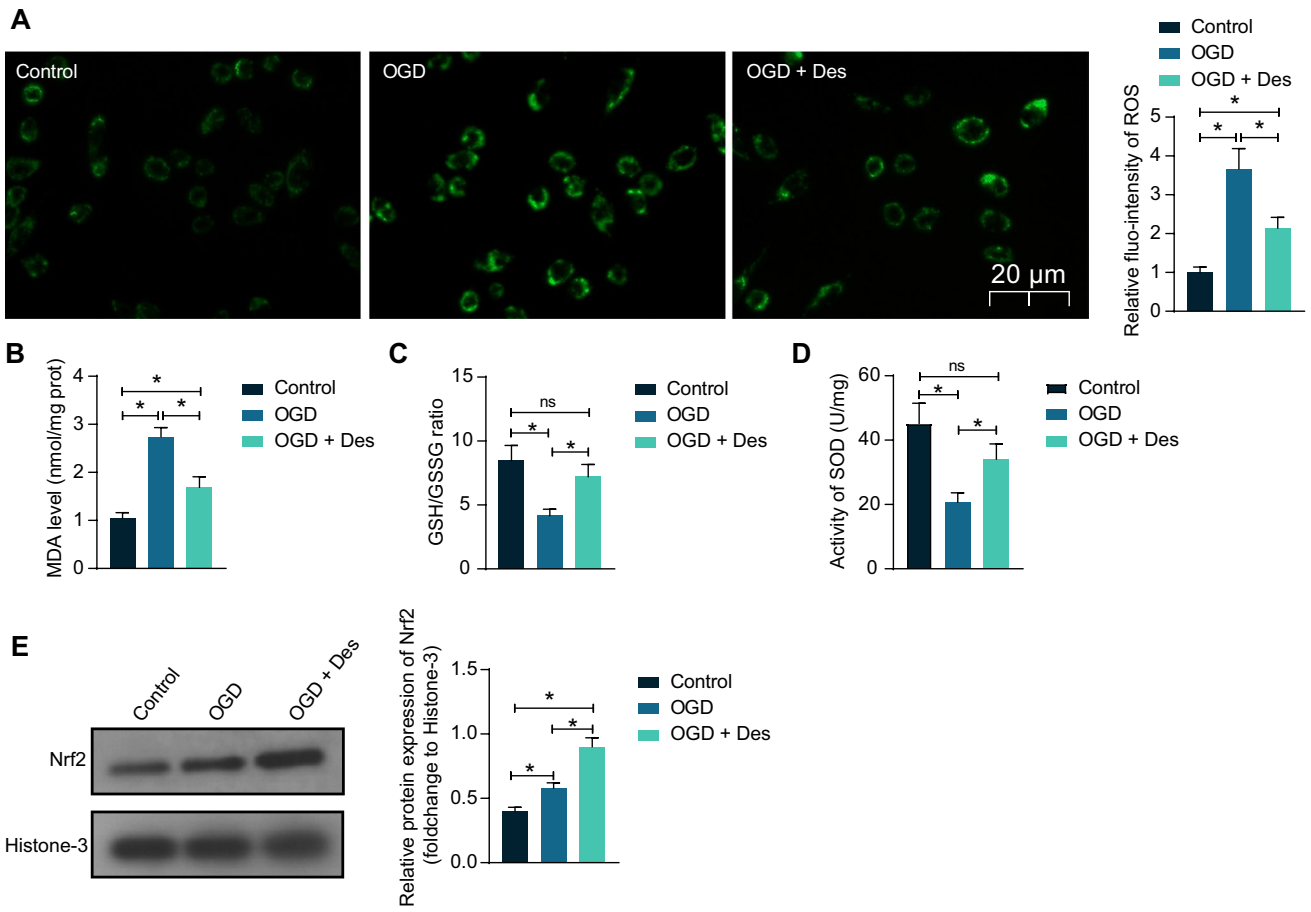

Fig. 2 Des alleviates OGD-induced oxidative stress in neurons. HT22 neuronal cells were subjected to OGD and then treated with Des. **A** ROS content in HT22 cells determined using an ROS fluorescent probe; **B** MDA content in HT22 cells analyzed using colorimetry; **C** GSH/GSSG ratio in HT22 cells; **D** SOD activity in HT22 cells measured using colorimetry; **E** nuclear protein level of Nrf2 in cells determined by WB analysis. Differences were analyzed using the one-way ANOVA (**A**–**E**). *$p < 0.05$, ns denotes to no significance

(Fig. 3A) using the STITCH system (http://stitch.embl.de/) (Fig. 3B). In addition, a GSE23158 dataset was downloaded (https://www.ncbi.nlm.nih.gov/geo/query/acc.cgi?acc=GSE23158) to analyze transcriptome alteration in mouse neurons following OGD (Fig. 3C). The significantly differentially expressed genes ($p < 0.01$) were cross-screened with the predicted proteins in Fig. 3B, and the one and only intersecting factor was obtained: Kcna1 (Fig. 3D). Of note, WB analysis showed that the Kcna1 protein level in HT22 cells was significantly decreased by OGD, which was restored after Des treatment to a level presenting no significance with the Control group (Fig. 3E). As the Kcna1 gene encodes voltage-gated potassium channel α subunit Kv1.1 and plays fundamental functions in maintaining neuronal firing while preventing hyperexcitability (Paulhus and Glasscock 2023), we surmised that Des might activate the Kv 1.1 channels to protect against neuronal injury.

Knockdown of Kcna1 negates the neuronal protective role of Des

To verify the involvement of Kcna1 in the neuronal protective events mediated by Des, the HT22 cells were pre-transfected with shRNA 1–3#, followed by OGD and Des treatments. Each of the three shRNA successfully decreased Kcna1 mRNA expression in cells. Among them, shRNA 2# showed a greater degree in suppression compared to shRNA 3#, though there was no statistical difference between the efficacy of shRNA 2# and shRNA 1#, or between shRNA 1# and shRNA 3# (Fig. 4A). Therefore, the shRNA 2# that exhibited the greatest knockdown efficacy was selected for subsequent use, termed KD-Kcna1. The KD-Kcna1 also significantly decreased the Kcna1 protein level in HT22 cells as well (Fig. 4B). Of note, in the setting of Kcna1 knockdown, the viability of HT22 cells was significantly reduced (Fig. 4C), along with increased LDH release (Fig. 4D) and increased cell apoptosis (Fig. 4E). Detection on the apoptosis-related proteins also

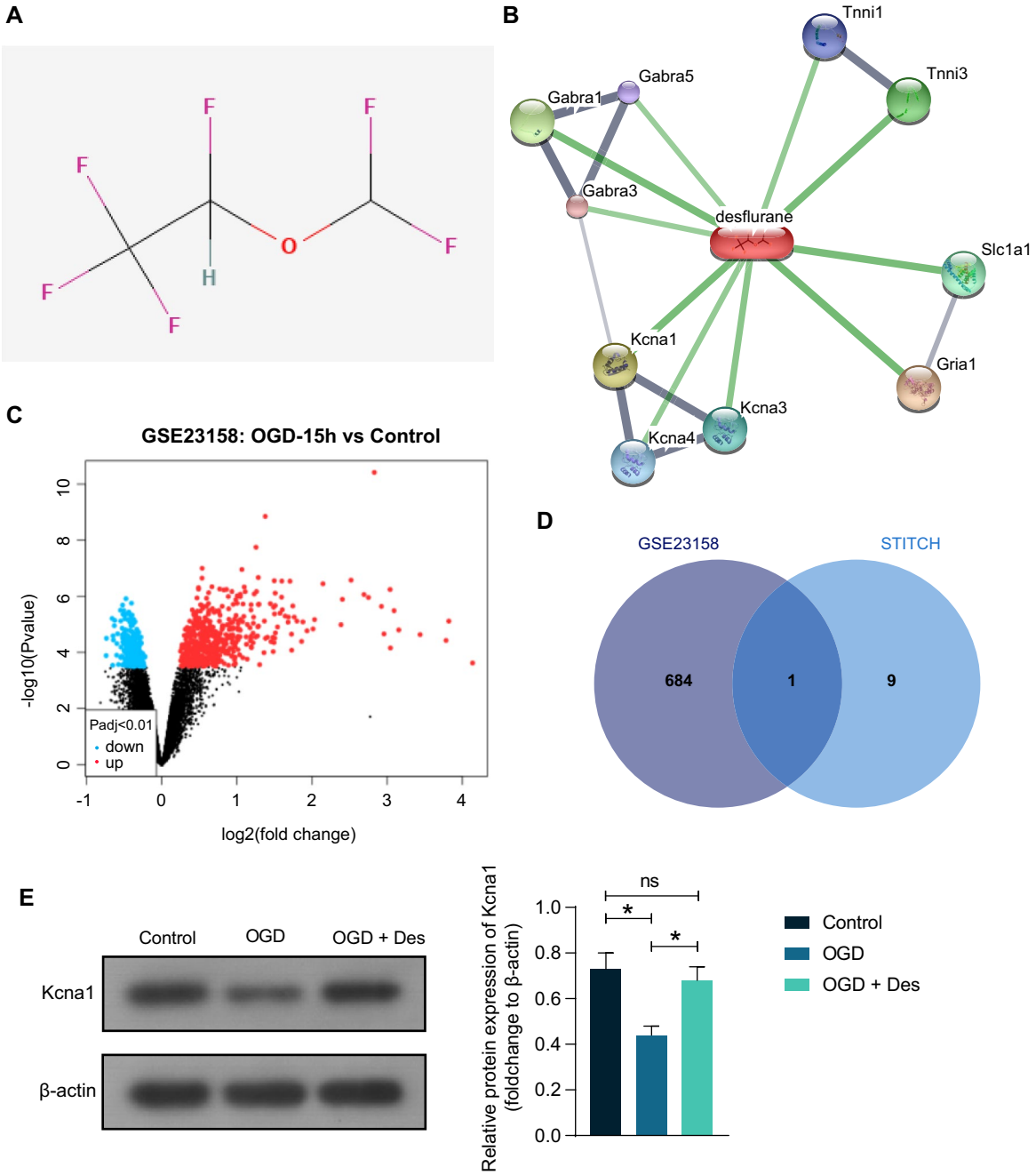

Fig. 3 Des restores Kcna1 expression decreased by OGD. **A** chemical structure of Des; **B** downstream proteins of Des predicted using the STITCH system; **C** transcriptome alteration in mouse neurons with or without OGD by analyzing the GSE23158 dataset; **D** intersection of the downstream proteins of Des and the significantly differentially expressed genes ($p < 0.01$) in the GSE23158 dataset; **E** Kcna1 protein level in HT22 cells after different treatments determined by WB analysis. Differences were analyzed using one-way ANOVA (**E**). *$p < 0.05$

showed that the Kcna1 knockdown significantly increased the Bax protein while downregulating the Bcl-2 protein (Fig. 4F). In addition, the accumulation of ROS (Fig. 4G) and MDA (Fig. 4H) was substantially increased, whereas the SOD activity (Fig. 4I), GSH/GSSG ratio (Fig. 4J), and the nuclear Nrf2 protein level (Fig. 4K) in cells were significantly decreased following Kcna1 knockdown. This evidence suggests that the neuronal protective effects of Des can be largely negated by Kcna1 silencing.

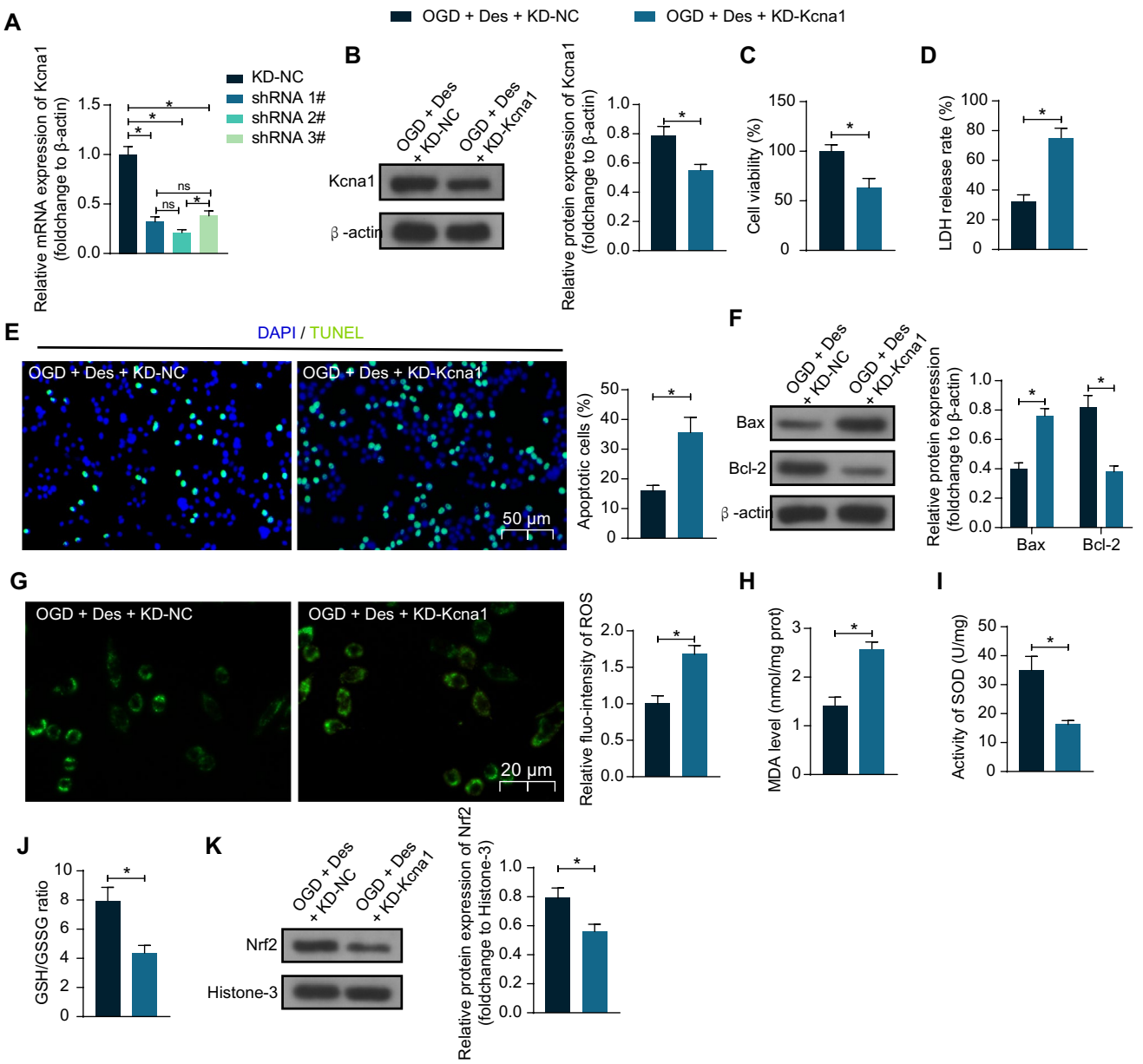

Fig. 4 Knockdown of Kcna1 negates the neuronal protective role of Des. HT22 neuronal cells were transfected with shRNA of Kcna1, followed by OGD procedure and Des treatment. **A** Kcna1 mRNA expression in HT22 cells after Kcna1 shRNA 1–3# transfection determined using RT-qPCR; **B** Kcna1 protein level in HT22 cells after Kcna1 shRNA transfection determined by WB analysis; **C** viability of HT22 cells measured by CCK-8 assay; **D** LDH release in cells to analyze the cytotoxicity; **E** apoptosis of HT22 cells analyzed using TUNEL assay; **F** protein levels of Bax and Bcl-2 in cells determined using WB analysis; **G**. ROS content in HT22 cells determined using an ROS fluorescent probe; **H** MDA content in HT22 cells analyzed using colorimetry; I, SOD activity in HT22 cells measured using colorimetry; **J** GSH/GSSG ratio in HT22 cells; **K** nuclear protein level of Nrf2 in cells determined by WB analysis. Differences were analyzed using the unpaired *t* test (**B**–**E**, **G**–**K**), the one-way ANOVA (**A**), or the two-way ANOVA (**F**). **p* < 0.05

Des activates the Kv1.1 channel to suppress hyperexcitability and loss of neurons

Subsequently, whether the neuronal signaling would be affected by OGD or Des was investigated. The RMP and the frequencies of spontaneous action potential (AP) firing and AP firing under 10 pA injection current of HT22 cells were determined. Importantly, it was found that the OGD process led to increased spike frequency (AP generation rate) (Fig. 5A), reduced neuronal repolarization (reduced RMP) (Fig. 5B), and increased generation of AP induced by 10 pA injection current (Fig. 5C). These alterations were partly reversed by Des treatment (with the spike frequency level still showing a significant increase compared to the

Control group, while RMP and inducive AP no longer showing a significant difference) (Fig. 5A–C). In addition, the K^+ currents were determined using the patch-clamp recordings to analyze the activity of the Kv1.1 channel. Importantly, the K^+ currents in HT22 cells were decreased by OGD treatment, which was partly restored following Des treatment (still showing a significant decrease compared to the Control group) (Fig. 5D). Representative electrophysiological data are presented in Supplementary Fig S1A–C. In addition, to inhibit the Kv1.1 channel, the HT22 cells were treated with DTx-K, followed by OGD and Des treatments. Indeed, the DTx-K significantly reduced the K^+ currents (Supplementary Fig S1C) (Fig. 5E). In this setting, the ROS and MDA contents in cells were increased (Fig. 5F and G), the GSH/GSSG ratio and SOD activity were decreased (Fig. 5H and I), and the nuclear protein of Nrf2 was reduced (Fig. 5J). Moreover, the DTx-K treatment increased the spike frequency (Fig. 5K), reduced repolarization (Fig. 5L), and increased the AP generation induced by 10 pA injection current (Fig. 5M) (Supplementary Fig S1A–B). This led to a decrease in neuronal viability (Fig. 5N) and an increase in neuronal apoptosis (Fig. 5O). Regarding the intracellular Ca^{2+} concentration, it was found that the Ca^{2+} concentration in HT22 cells was increased by OGD challenge, reduced by Des treatment, and increased again by the DTx-K treatment (Fig. 5P).

Discussion

While there is a pressing requirement for neuroprotective measures in the face of a stroke, the precise intricacies governing neuronal death amid ischemic stroke continue to be veiled in uncertainty. This lack of clarity has consequently imposed constraints upon the scope for advancing drug development efforts (Tuo et al. 2022). This study reports that Des protects neurons from oxidative stress and cell apoptosis under OGD-stressed condition. Most of all, the protective function entails the modulation of neuronal electrophysiology through Kcna1 and the Kv1.1 channel.

Existing evidence has demonstrated the potent function of volatile anesthetics in alleviating infarct volume and improving outcome of ischemic stroke, as well as in reducing incidence and severity of postoperative ischemic stroke (Raub et al. 2021). In a clinical trial of 313 ischemic stroke patients receiving endovascular thrombectomy, administration of volatile anesthetics (Des or sevoflurane) in 254 (81%) patients led to more significant stroke alleviation and better prognosis compared to the others administrated with intravenous propofol (Diprose et al. 2021). Isoflurane and sevoflurane are among the most investigated volatile anesthetics with clear neuroprotective properties in experimental animal and cellular models of ischemic stroke/OGD or reperfusion injury (Cai et al. 2021; Chen et al. 2022a; Kim et al. 2015; Peng et al. 2011; Shpetko et al. 2023; Wang et al. 2016, 2018; Zhou et al. 2010). Des is one of the major volatile anesthetics in clinical practice as well with few side effects, yet its application is less due to the economic disadvantage (Deng et al. 2014). Importantly, Des has been found to has a similar protective function like sevoflurane and isoflurane in OGD-challenged human neuron-like cells by suppressing the glycogen synthase kinase 3β signaling (Lin et al. 2011). A previous publication reports that Des presented a greater protective effect than halothane in cerebral ischemia (Haelewyn et al. 2003). Notably, in this study, we found that the Des post-treatment significantly promoted viability of OGD-challenged mouse hippocampal neuronal cell line HT22 while reducing LDH release and cell apoptosis. Similarly, Lin et al. reported that post-treatment of Des significantly reduced LDH release in OGD-challenged human neuron-like SH-SY5Y cells (Lin et al. 2011). Notably, we found that pre-treatment of Des did not significantly prevent HT22 cells from OGD-induced injury. This was consistent with findings in a previous study (Schallner et al. 2014), which also indicates that Des is more likely to exert an alleviating effect rather than a preventive effect against OGD. Additionally, one of the primary mechanisms underlying neuronal death following OGD is the induction of mitochondrial impairment and oxidative stress (Almeida et al. 2002; Gouix et al. 2014). Indeed, we found that the Des treatment reduced oxidative stress and activated the antioxidant defense mechanism in the OGD-challenged HT22 cells, as manifested by decreased ROS and MDA contents, restored SOD activity, GSH/GSSG ratio, and increased nuclear translocation of Nrf2 protein.

Then, when probing the molecular underpinning for the neuroprotective effect of Des, we obtained Kcna1 as a promising target after integrated bioinformatics analyses. The Kcna1 gene encodes the Kv1.1 channel, a K^+-selective channel widely expressed in the central nervous system (Servettini et al. 2023). The Kv channels play crucial roles in various functions of cells, such as maintenance of membrane potential, repolarization of the AP, and regulation of neuronal firing patterns as well as cell proliferation and apoptosis (Pardo 2004; Wonderlin and Strobl 1996; Yi et al. 2001). When a neuron receives a signal, it depolarizes, causing a change in the electrical potential across its membrane, which triggers the opening of voltage-gated ion channels, including Kv1.1 (Gera et al. 2015; Wang et al. 2017). The Kv1.1 channel regulate the outward flow of K^+, which helps repolarize the neuron, restoring its RMP and allowing it to fire another AP (Abbott 2006; Speake et al. 2004; Yang 2022). Therefore, dysregulation of Kcan1 (Kv1.1) may impair the ability of neurons to regulate their firing properly, leading to neuronal hyperexcitability and neurological disorders such as episodic ataxia type 1 (Servettini et al. 2023). Importantly,

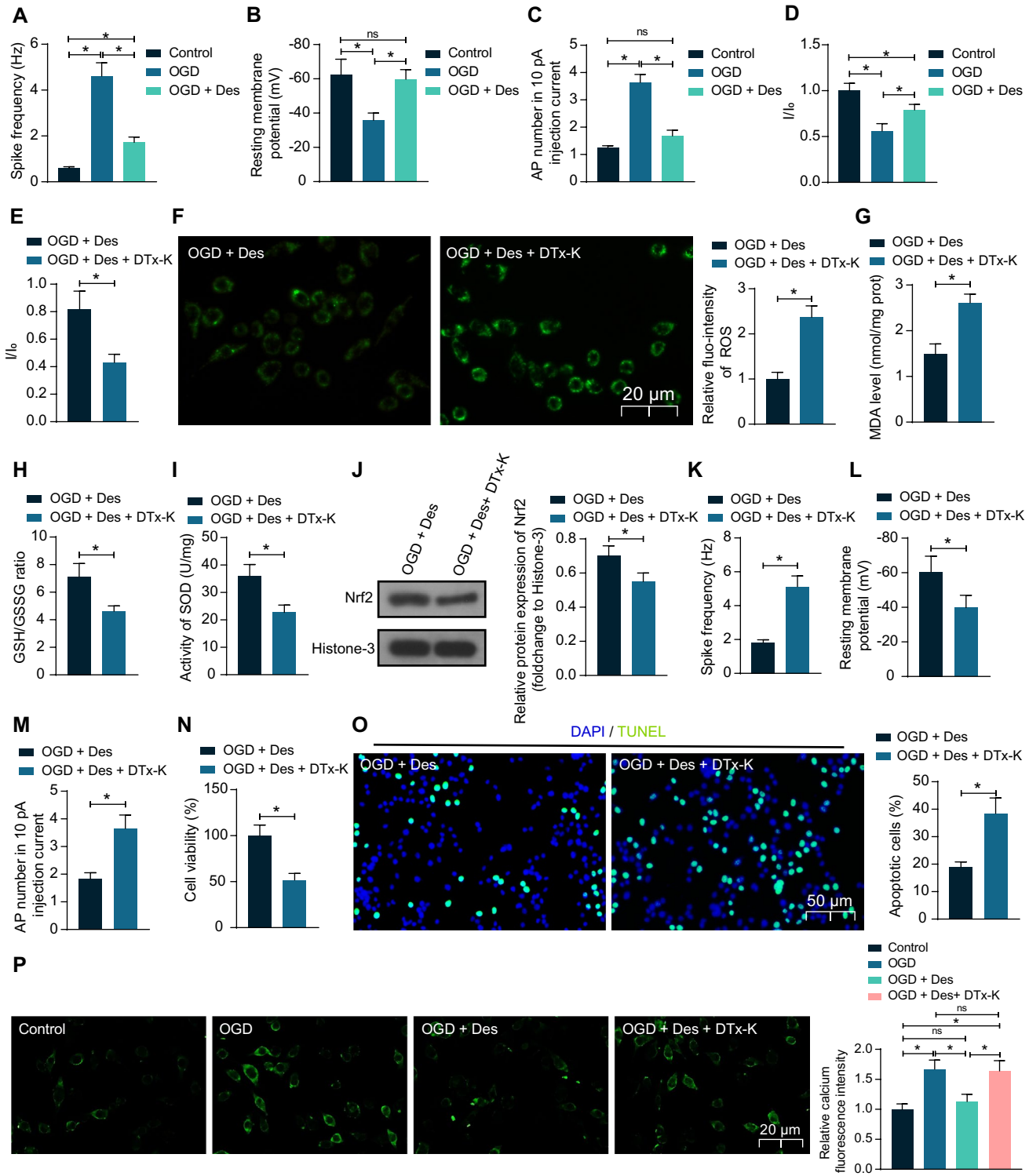

in this study, we found that the OGD challenge led increased the frequency of spontaneous AP firing and 10 pA current-induced AP firing of neurons while reducing RMP and the K^+ currents. Such alterations in neuronal signaling following OGD challenge have also observed in previous publications (Wang et al. 2019). This indicates a hyperexcitability status of neurons, which can lead to neuronal apoptosis and injury (Bhat et al. 2022; Chen et al. 2022b). Consistently, we found that the OGD challenge increased the intracellular Ca^{2+} levels in neurons, which are known factors leading to excitotoxicity and death of neurons (Harris and Harris 2018; Mattson et al. 1992). Importantly, we found that the

◂**Fig. 5** Des activates the Kv1.1 channel to suppress hyperexcitability and loss of neurons. HT22 neuronal cells were subjected to OGD and then treated with Des. A-C, spike frequency (**A**), RMP (**B**), and generation of AP induced by 10 pA injection current (**C**) in HT22 cells following OGD and Des treatment determined using patch-clamp technique; **D** K^+ currents in HT22 cells following OGD and Des treatment determined using patch-clamp technique; **E** K^+ currents in HT22 cells after DTx-K treatment examined using patch-clamp technique; **F** ROS content in HT22 cells after DTx-K treatment determined using an ROS fluorescent probe; **G** MDA content in HT22 cells after DTx-K treatment analyzed using colorimetry; **H** GSH/GSSG ratio in HT22 cells after DTx-K treatment; **I**, SOD activity in HT22 cells after DTx-K treatment measured using colorimetry; **J** nuclear protein level of Nrf2 in cells after DTx-K treatment determined by WB analysis; **K–M** spike frequency (**K**), RMP (**L**), and generation of AP induced by 10 pA injection current (**M**) in HT22 cells after DTx-K treatment determined using patch-clamp technique; **N** viability of HT22 cells after DTx-K treatment determined by CCK-8 assay; **O** apoptosis of HT22 cells after DTx-K treatment examined using TUNEL assay. **P** Intracellular Ca^{2+} concentration determined by the Fluo-3 AM staining. Differences were compared by the one-way ANOVA (**A–D**, **P**) or by the unpaired *t* test (**E–O**). $^*p < 0.05$

Des treatment restored the Kcna1 protein level in neurons and suppressed the neuronal hyperexcitability according to the electrophysiological data. However, pharmacological inhibition of the Kv1.1 channel using DTx-K reversed the protective effects of Des against OGD-induced Ca^{2+} accumulation and neuronal hyperexcitability. This was partly in line with the previous findings by Begum et al., where acute blockade of Kv1.1 channels using DTx-K resulted in an increase in action potential-evoked Ca^{2+} influx (Begum et al. 2016). This ample evidence indicates that indicate that the Kcna1/Kv1.1 channel activation is, at least in part, implicated in the neuroprotective events mediated by Des upon OGD challenge.

Here we found that the Des prevented hyperexcitability and apoptosis of mouse hippocampal neurons. In fact, Des has been reported to affect various types of neurons. As mentioned earlier, it has been found to significantly reduce LDH release in human neuron-like SH-SY5Y cells deprived of oxygen and glucose (Lin et al. 2011). When inducing unconsciousness, Des has been reported to present a preferential suppression of feedback between secondary and primary visual cortex (Hudetz et al. 2020). At anesthetic concentrations, sevoflurane and Des exhibited a reduction in the occurrence of APs within the dorsal horn of rats (Inada et al. 2020). Simultaneously, they attenuated the excitatory postsynaptic currents in substantia gelatinosa neurons during pinch stimulation, leading to a decline in both spontaneous and miniature excitatory postsynaptic currents (Inada et al. 2020). Additionally, desflurane has been found to make firing of Granule cells more regular without abolishing the cells' capacity of eliciting spikes (Mapelli et al. 2015). This ample evidence indicates the important regulatory roles of Des in various types of neurons. However, whether certain neuronal subtypes or regions display a heightened reactivity to Des requires further investigation. Concerning the interplay of Des or alternative volatile anesthetics with Kv channels, available indications propose that anesthetics selectively influence Kv1 channels within a network. This is evident when ShK, an inhibitor targeting Kv1.1, Kv1.3, and Kv1.6 channels, is introduced into the central medial thalamic nucleus, resulting in the arousal of rodents anesthetized with sevoflurane (Lioudyno et al. 2013). Sevoflurane, isoflurane, and/or Des have been demonstrated to accelerate activation of the Kv1.3 channel, slowed deactivation kinetics of Kv1.3 channels, and potentiated potassium currents, thereby suppressing neuronal excitability in the CMT (Lioudyno et al. 2013). However, in the study by Friederich et al., several volatile anesthetics at clinical concentrations were found to inhibit human Kv3 channels in SH-SY5Y cells, and enflurane was found to inhibit Kv1.1 channels in 293 T cells (Friederich et al. 2001). This discrepancy indicates that the function of anesthetics in Kv channels can vary depending on certain cellular or stimulation contexts, and the detailed mechanisms warrant further investigation.

Conclusions

In conclusion, this study provides evidence that Des improves neuronal electrical activity and alleviates OGD-induced neuronal injury by activating the Kcna1-dependent Kv1.1 channel (Fig. 6). The findings contribute new insights into the insights underlying the neuroprotective functions of volatile anesthetics. However, it is essential to acknowledge several limitations in the present study. Firstly, while low or moderate concentrations of anesthetics commonly present neuroprotective properties, a high concentration might induce developmental neurotoxicity (Chen et al. 2018). This study only administered a single dose of Des, and thus, its dose-dependent effects or potential neurotoxicity remain unclear. Furthermore, the mechanism through which the Kv 1.1 channel regulates oxidative stress remains uncertain but represents an intriguing avenue for further exploration. Additionally, due to time, ethical, and financial constraints, we did not conduct in vivo animal experiments to validate the in vitro findings. This limitation may restrict the clinical translational value of our present discoveries. Addressing these issues will be a focal point in our future research endeavors.

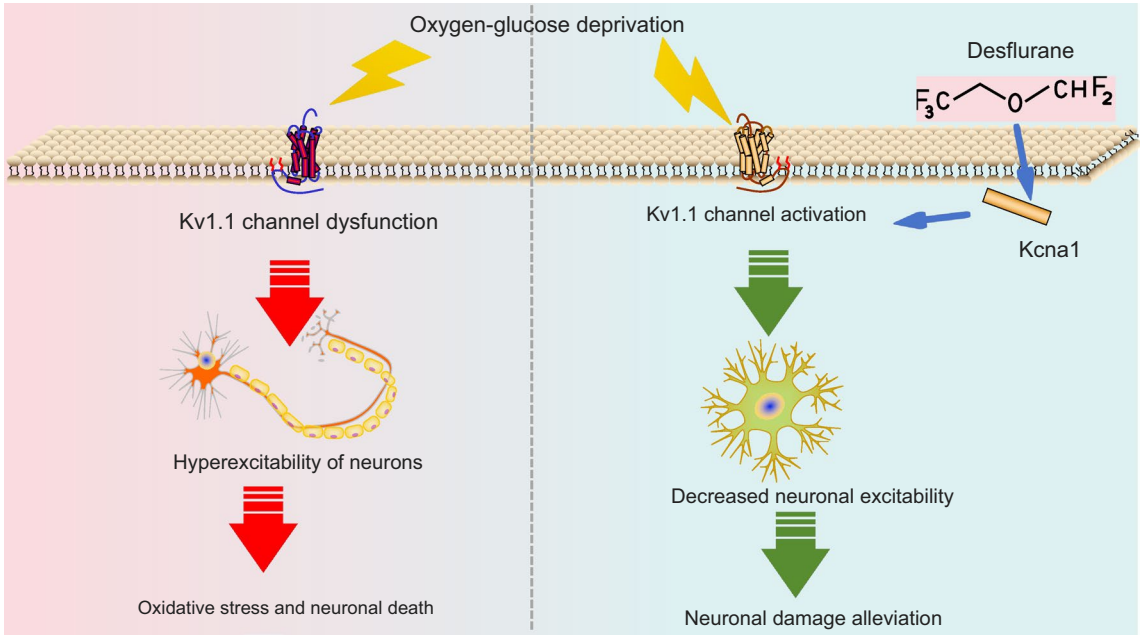

Fig. 6 Graphical abstract. Des improves neuronal electrical activity, alleviates OGD-induced hyperexcitability neurons by activating the Kcna1-dependent Kv1.1 channel, therefore alleviating neuronal damage and loss

Supplementary Information The online version contains supplementary material available at https://doi.org/10.1007/s00221-023-06764-w.

Acknowledgements None.

Author contributions XLN performed experiments and wrote the manuscript; XYY performed experiments and collected data; QQY performed experiments and statistical analysis; XHS conceived the idea and designed the study; SS designed and supervised the study, and revised the manuscript. All authors have read and approved the manuscript.

Funding None.

Data availability The datasets generated during and/or analyzed during the current study are available from the corresponding author on reasonable request.

Declarations

Conflict of interest The authors declare that there is no conflict of interest regarding the publication of this paper.

References

Abbott GW (2006) Molecular mechanisms of cardiac voltage-gated potassium channelopathies. Curr Pharm Des 12:3631–3644. https://doi.org/10.2174/138161206778522065

Almeida A, Delgado-Esteban M, Bolanos JP, Medina JM (2002) Oxygen and glucose deprivation induces mitochondrial dysfunction and oxidative stress in neurones but not in astrocytes in primary culture. J Neurochem 81:207–217. https://doi.org/10.1046/j.1471-4159.2002.00827.x

Begum R, Bakiri Y, Volynski KE, Kullmann DM (2016) Action potential broadening in a presynaptic channelopathy. Nat Commun 7:12102. https://doi.org/10.1038/ncomms12102

Bhat MA, Esmaeili A, Neumann E, Balakrishnan K, Benke D (2022) Targeting the interaction of GABA(B) receptors with CHOP after an ischemic insult restores receptor expression and inhibits progressive neuronal death. Front Pharmacol 13:870861. https://doi.org/10.3389/fphar.2022.870861

Brioni JD, Varughese S, Ahmed R, Bein B (2017) A clinical review of inhalation anesthesia with sevoflurane: from early research to emerging topics. J Anesth 31:764–778. https://doi.org/10.1007/s00540-017-2375-6

Cai M et al (2021) Sevoflurane preconditioning protects experimental ischemic stroke by enhancing anti-inflammatory microglia/macrophages phenotype polarization through GSK-3beta/Nrf2 pathway. CNS Neurosci Ther 27:1348–1365. https://doi.org/10.1111/cns.13715

Chen X et al (2018) Neonatal exposure to low-dose (1.2%) sevoflurane increases rats' hippocampal neurogenesis and synaptic plasticity in later life. Neurotox Res 34:188–197. https://doi.org/10.1007/s12640-018-9877-3

Chen C, Zuo J, Zhang H (2022a) Sevoflurane post-treatment mitigates oxygen-glucose deprivationinduced pyroptosis of hippocampal neurons by regulating the Mafb/DUSP14 axis. Curr Neurovasc Res 19:245–254. https://doi.org/10.2174/1567202616966220802104426

Chen X, Zhang J, Wang K (2022b) Inhibition of intracellular proton-sensitive Ca(2+)-permeable TRPV3 channels protects against ischemic brain injury. Acta Pharm Sin B 12:2330–2347. https://doi.org/10.1016/j.apsb.2022.01.001

Cheng A, Lu Y, Huang Q, Zuo Z (2019) Attenuating oxygen-glucose deprivation-caused autophagosome accumulation may be involved in sevoflurane postconditioning-induced protection in human neuron-like cells. Eur J Pharmacol 849:84–95. https://doi.org/10.1016/j.ejphar.2019.01.051

Deng J et al (2014) Neuroprotective gases–fantasy or reality for clinical use? Prog Neurobiol 115:210–245. https://doi.org/10.1016/j.pneurobio.2014.01.001

Diprose WK et al (2021) Intravenous propofol versus volatile anesthetics for stroke endovascular thrombectomy. J Neurosurg Anesthesiol 33:39–43. https://doi.org/10.1097/ANA.0000000000000639

Friederich P, Benzenberg D, Trellakis S, Urban BW (2001) Interaction of volatile anesthetics with human Kv channels in relation to clinical concentrations. Anesthesiology 95:954–958. https://doi.org/10.1097/00000542-200110000-00026

Gera N, Yang A, Holtzman TS, Lee SX, Wong ET, Swanson KD (2015) Tumor treating fields perturb the localization of septins and cause aberrant mitotic exit. PLoS ONE 10:e0125269. https://doi.org/10.1371/journal.pone.0125269

Gouix E, Buisson A, Nieoullon A, Kerkerian-Le Goff L, Tauskela JS, Blondeau N, Had-Aissouni L (2014) Oxygen glucose deprivation-induced astrocyte dysfunction provokes neuronal death through oxidative stress. Pharmacol Res 87:8–17. https://doi.org/10.1016/j.phrs.2014.06.002

Haelewyn B, Yvon A, Hanouz JL, MacKenzie ET, Ducouret P, Gerard JL, Roussel S (2003) Desflurane affords greater protection than halothane against focal cerebral ischaemia in the rat. Br J Anaesth 91:390–396. https://doi.org/10.1093/bja/aeg186

Hao L, Zou Z, Tian H, Zhang Y, Zhou H, Liu L (2014) Stem cell-based therapies for ischemic stroke. Biomed Res Int 2014:468748. https://doi.org/10.1155/2014/468748

Harris SA, Harris EA (2018) Molecular mechanisms for herpes simplex virus type 1 pathogenesis in Alzheimer's disease. Front Aging Neurosci 10:48. https://doi.org/10.3389/fnagi.2018.00048

Hudetz AG, Pillay S, Wang S, Lee H (2020) Desflurane anesthesia alters cortical layer-specific hierarchical interactions in rat cerebral cortex. Anesthesiology 132:1080–1090. https://doi.org/10.1097/ALN.0000000000003179

Inada Y, Funai Y, Yamasaki H, Mori T, Nishikawa K (2020) Effects of sevoflurane and desflurane on the nociceptive responses of substantia gelatinosa neurons in the rat spinal cord dorsal horn: an in vivo patch-clamp analysis. Mol Pain 16:1744806920903149. https://doi.org/10.1177/1744806920903149

Katan M, Luft A (2018) Global burden of stroke. Semin Neurol 38:208–211. https://doi.org/10.1055/s-0038-1649503

Khatibi NH et al (2011) Isoflurane posttreatment reduces brain injury after an intracerebral hemorrhagic stroke in mice. Anesth Analg 113:343–348. https://doi.org/10.1213/ANE.0b013e31821f9524

Kim EJ, Kim SY, Lee JH, Kim JM, Kim JS, Byun JI, Koo BN (2015) Effect of isoflurane post-treatment on tPA-exaggerated brain injury in a rat ischemic stroke model. Korean J Anesthesiol 68:281–286. https://doi.org/10.4097/kjae.2015.68.3.281

Kumar S, Singh PR, Srivastava VK, Khan MP, Singh MK, Shyam R (2023) Recovery and post-operative analgesic efficacy from fentanyl-versus dexmedetomidine-based anesthesia in head and neck cancer surgery: a prospective comparative trial. Natl J Maxillofac Surg 14:130–135. https://doi.org/10.4103/njms.njms_3_22

Lakhan SE, Kirchgessner A, Hofer M (2009) Inflammatory mechanisms in ischemic stroke: therapeutic approaches. J Transl Med 7:97. https://doi.org/10.1186/1479-5876-7-97

Li M, Peng J, Wang MD, Song YL, Mei YW, Fang Y (2014) Passive movement improves the learning and memory function of rats with cerebral infarction by inhibiting neuron cell apoptosis. Mol Neurobiol 49:216–221. https://doi.org/10.1007/s12035-013-8512-9

Lin D, Li G, Zuo Z (2011) Volatile anesthetic post-treatment induces protection via inhibition of glycogen synthase kinase 3beta in human neuron-like cells. Neuroscience 179:73–79. https://doi.org/10.1016/j.neuroscience.2011.01.055

Lioudyno MI et al (2013) Shaker-related potassium channels in the central medial nucleus of the thalamus are important molecular targets for arousal suppression by volatile general anesthetics. J Neurosci 33:16310–16322. https://doi.org/10.1523/JNEUROSCI.0344-13.2013

Malhotra P, Mychaskiw G, Rai A (2013) Desflurane versus opioid anesthesia for cardiac shunt procedures in infants with cyantoic congential heart disease. Anesth Pain Med 3:191–197. https://doi.org/10.5812/aapm.9511

Mao R, Zong N, Hu Y, Chen Y, Xu Y (2022) Neuronal death mechanisms and therapeutic strategy in ischemic stroke. Neurosci Bull 38:1229–1247. https://doi.org/10.1007/s12264-022-00859-0

Mapelli J et al (2015) The effect of desflurane on neuronal communication at a central synapse. PLoS ONE 10:e0123534. https://doi.org/10.1371/journal.pone.0123534

Mattson MP, Cheng B, Davis D, Bryant K, Lieberburg I, Rydel RE (1992) beta-Amyloid peptides destabilize calcium homeostasis and render human cortical neurons vulnerable to excitotoxicity. J Neurosci 12:376–389. https://doi.org/10.1523/JNEUROSCI.12-02-00376.1992

Miller AP, Navar AM, Roubin GS, Oparil S (2016) Cardiovascular care for older adults: hypertension and stroke in the older adult. J Geriatr Cardiol 13:373–379. https://doi.org/10.11909/j.issn.1671-5411.2016.05.001

Morone G, Pichiorri F (2023) Post-stroke rehabilitation: challenges and new perspectives. J Clin Med 12. https://doi.org/10.3390/jcm12020550

Pardo LA (2004) Voltage-gated potassium channels in cell proliferation. Physiology (bethesda) 19:285–292. https://doi.org/10.1152/physiol.00011.2004

Paulhus K, Glasscock E (2023) Novel genetic variants expand the functional, molecular, and pathological diversity of KCNA1 channelopathy. Int J Mol Sci 24. https://doi.org/10.3390/ijms24108826

Peng S et al (2011) Sevoflurane postconditioning ameliorates oxygen-glucose deprivation-reperfusion injury in the rat hippocampus. CNS Neurosci Ther 17:605–611. https://doi.org/10.1111/j.1755-5949.2010.00193.x

Raub D et al (2021) Effects of volatile anesthetics on postoperative ischemic stroke incidence. J Am Heart Assoc 10:e018952. https://doi.org/10.1161/JAHA.120.018952

Robinson T, Zaheer Z, Mistri AK (2011) Thrombolysis in acute ischaemic stroke: an update. Ther Adv Chronic Dis 2:119–131. https://doi.org/10.1177/2040622310394032

Schallner N, Ulbrich F, Engelstaedter H, Biermann J, Auwaerter V, Loop T, Goebel U (2014) Isoflurane but not sevoflurane or desflurane aggravates injury to neurons in vitro and in vivo via p75NTR-NF-kB activation. Anesth Analg 119:1429–1441. https://doi.org/10.1213/ANE.0000000000000488

Schifilliti D, Grasso G, Conti A, Fodale V (2010) Anaesthetic-related neuroprotection: intravenous or inhalational agents? CNS Drugs 24:893–907. https://doi.org/10.2165/11584760-000000000-00000

Servettini I et al. (2023) An activator of voltage-gated K(+) channels Kv1.1 as a therapeutic candidate for episodic ataxia type 1. Proc Natl Acad Sci USA 120:e2207978120. https://doi.org/10.1073/pnas.2207978120

Shah NH, Aizenman E (2014) Voltage-gated potassium channels at the crossroads of neuronal function, ischemic tolerance, and neurodegeneration. Transl Stroke Res 5:38–58. https://doi.org/10.1007/s12975-013-0297-7

Shpetko YY, Filippenkov IB, Denisova AE, Stavchansky VV, Gubsky LV, Limborska SA, Dergunova LV (2023) Isoflurane anesthesia's impact on gene expression patterns of rat brains in an ischemic stroke model. Genes (Basel) 14. https://doi.org/10.3390/genes14071448

Speake T, Kibble JD, Brown PD (2004) Kv1.1 and Kv1.3 channels contribute to the delayed-rectifying K+ conductance in rat choroid plexus epithelial cells. Am J Physiol Cell Physiol 286:C611-620. https://doi.org/10.1152/ajpcell.00292.2003

Tuo QZ, Zhang ST, Lei P (2022) Mechanisms of neuronal cell death in ischemic stroke and their therapeutic implications. Med Res Rev 42:259–305. https://doi.org/10.1002/med.21817

Vizuete JA, Pillay S, Diba K, Ropella KM, Hudetz AG (2012) Monosynaptic functional connectivity in cerebral cortex during wakefulness and under graded levels of anesthesia. Front Integr Neurosci 6:90. https://doi.org/10.3389/fnint.2012.00090

Wang H, Li P, Xu N, Zhu L, Cai M, Yu W, Gao Y (2016) Paradigms and mechanisms of inhalational anesthetics mediated neuroprotection against cerebral ischemic stroke. Med Gas Res 6:194–205. https://doi.org/10.4103/2045-9912.196901

Wang L, Lu SR, Wen J (2017) Recent advances on neuromorphic systems using phase-change materials. Nanoscale Res Lett 12:347. https://doi.org/10.1186/s11671-017-2114-9

Wang S, Li Y, Wei J, Li P, Yang Q (2018) Sevoflurane preconditioning induces tolerance to brain ischemia partially via inhibiting thioredoxin-1 nitration. BMC Anesthesiol 18:171. https://doi.org/10.1186/s12871-018-0636-z

Wang X et al (2019) TRPV1 translocated to astrocytic membrane to promote migration and inflammatory infiltration thus promotes epilepsy after hypoxic ischemia in immature brain. J Neuroinflammation 16:214. https://doi.org/10.1186/s12974-019-1618-x

Wonderlin WF, Strobl JS (1996) Potassium channels, proliferation and G1 progression. J Membr Biol 154:91–107. https://doi.org/10.1007/s002329900135

Yang F (2022) A gating mechanism of K2P channels by their selectivity filter. J Mol Cell Biol 14. https://doi.org/10.1093/jmcb/mjac018

Yi BA, Minor DL Jr, Lin YF, Jan YN, Jan LY (2001) Controlling potassium channel activities: interplay between the membrane and intracellular factors. Proc Natl Acad Sci U S A 98:11016–11023. https://doi.org/10.1073/pnas.191351798

Zhong W, Huang Q, Zeng L, Hu Z, Tang X (2019) Caveolin-1 and MLRs: a potential target for neuronal growth and neuroplasticity after ischemic stroke. Int J Med Sci 16:1492–1503. https://doi.org/10.7150/ijms.35158

Zhou Y, Lekic T, Fathali N, Ostrowski RP, Martin RD, Tang J, Zhang JH (2010) Isoflurane posttreatment reduces neonatal hypoxic-ischemic brain injury in rats by the sphingosine-1-phosphate/phosphatidylinositol-3-kinase/Akt pathway. Stroke 41:1521–1527. https://doi.org/10.1161/STROKEAHA.110.583757